Heat conduction engineering in pillar-based phononic crystals

Roman Anufriev and Masahiro Nomura

Phys. Rev. B **95**, 155432 — Published 20 April 2017

DOI: 10.1103/PhysRevB.95.155432

Heat conduction engineering in pillar-based phononic crystals

Roman Anufriev[1,*] and Masahiro Nomura[1,2,*]

[1]*Institute of Industrial Science, University of Tokyo, Tokyo, 153-8505, Japan*

[2]*PRESTO, Japan Science and Technology Agency, Saitama, 332–0012, Japan*

*Emails: r.l.anufriev@gmail.com, nomura@iis.u-tokyo.ac.jp

Pillar-based phononic crystals belong to a class of acoustic metamaterials that can control heat conduction based on the design of the structure. In this work, we systematically investigate how various parameters of pillar-based phononic crystals affect thermal conductance at low temperatures. We find that the lowest thermal conductance is achieved when the pillars are short, have a large radius, a long period, and are made of materials with few local resonances, whereas pillar with many local resonances can on the contrary increase thermal conductance. We argue that properly designed pillar-based phononic crystals can serve as an alternative to conventional hole-based phononic crystals because local resonances in pillars introduce additional degree of freedom, which allows not only suppressing but also enhancing heat conduction. Moreover, we propose hybrid hole/pillar-based phononic crystals that can further reduce thermal conductance.

I. INTRODUCTION

Propagation of phonons in solids can be effectively controlled by phononic crystals (PnCs), a class of artificial nanostructures in which the phonon dispersion can be engineered via structural design [1,2]. PnCs proposed for most applications are typically two-dimensional [3] and consist of periodic arrays of either holes in a membrane (hole-based PnCs) or pillars (e.g. nanowires or dots) on top of a membrane (pillar-based PnCs) [4–6]. The geometrical parameters of such PnCs can be tuned to control phonon interference [7] that occurs when phonons are coherently (elastically) scattered on the periodic interfaces [2]. In addition, pillars on top of the membrane can act as resonators [8–13] that create states localized in the pillars – the local resonances (LRs).

Whereas hole-based PnCs have received considerable attention and have proven promising for the control of both heat and sound [1,2], pillar-based PnCs have been mostly considered with regard to

sound. Indeed, most theoretical [10,13–17] and experimental [5,8,17–20] studies on pillar-based PnCs have focused on the formation of acoustic bandgaps – frequency ranges in which phonons cannot propagate through the PnC. Although the bandgaps are useful for various applications [14,16,21,22], they are of little use for heat conduction engineering because they cover only a narrow range of rather low frequencies, whereas heat consists of phonons with frequencies within a much wider range [7,23]. However, phonon interference in PnCs changes phonon dispersion even at higher frequencies [5,7] as long as phonon scattering remains coherent so that the interference can develop. Thus, pillar-based PnCs can potentially control heat conduction. Recent molecular dynamics simulations [9,24–26] predicted a more than 50% reduction in the thermal conductivity of pillar-based PnCs compared to that of membranes without pillars; this reduction has been tentatively attributed to the flattening of phonon dispersion caused by the LRs in pillars.

In this work, we seek to understand the processes behind the suppression of heat conduction in pillar-based PnCs and systematically investigate how various geometrical and material parameters affect the presence of LRs, and consequently, the thermal conductance, within the purely coherent regime. We find that the strongest suppression of heat conduction is achieved when the pillars have a small height, large radius, long period, and are made of materials with few LRs. In general, we show that properly designed pillar-based PnCs can suppress heat conduction as efficiently as their hole-based counterparts. Moreover, we introduce hybrid hole/pillar-based PnCs that can reduce thermal conductance more than hole- or pillar-based PnCs.

II. SIMULATION OF PHONONIC CRYSTALS

Our pillar-based PnCs consist of a two-dimensional array of pillars arranged in a hexagonal lattice on top of a silicon membrane, as shown in Figure 1. To simulate such periodic structure, we consider a unit cell, shown in Figure 1(c), with Floquet periodic boundary conditions applied in the x–y plane. As long as phonon wavelengths are longer than the atomic scale, we can apply the classical theory of

elasticity to describe phonons as elastic waves. In this work, we assume that materials are isotropic and that the pillars and the membrane have atomically perfect interface without strain. Thus, the phonon dispersion, $\omega(k)$, can be obtained from the elastodynamic wave equation: $\mu\nabla^2\mathbf{u} + (\mu + \lambda)\nabla(\nabla\cdot\mathbf{u}) = -\rho\omega^2\mathbf{u}$, with $\mathbf{u}$ as the displacement vector, ρ as the mass density, and λ and μ as the Lamé parameters of considered materials (Appendix A). To numerically solve this equation, we use the finite element method, implemented using Comsol Multiphysics® v5.1, and mesh the unit cell with finite elements smaller in size than the phonon wavelengths at the considered temperatures (Appendix B). To obtain the full phonon dispersion $\omega(k)$ in the entire first Brillouin zone, we search for eigenfrequencies (ω) at 100 k-points (Appendix B) on each side of the irreducible triangle of the first Brillouin zone and then interpolate (Appendix C) the solutions inside the triangle. The dispersion of a reference membrane without pillars is obtained from analytic Rayleigh–Lamb equations [27]. Additionally, we calculate the number of LRs in pillars by simulating a single pillar with a fixed bottom boundary and counting the number of eigenfrequencies below 80 GHz.

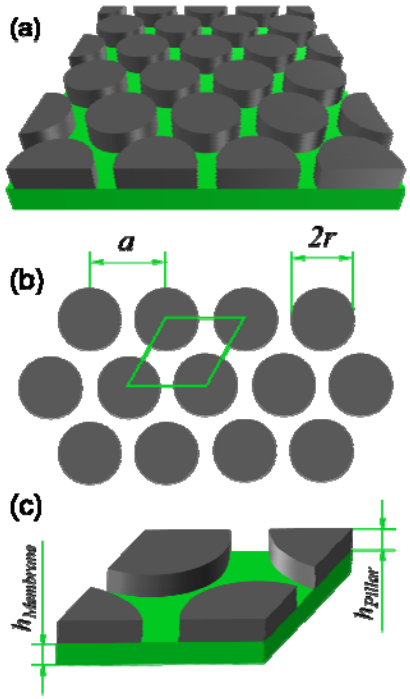

FIG. 1. (Color online) (a) Schematic of a pillar-based PnC consisting of silicon membrane and an array of pillars. (b) The hexagonal lattice of pillars and (c) a simulated unit cell.

The thermal conductance (G) at a given temperature (T) can be calculated from the dispersion ω(k) as (Appendix D):

$$G(T) = \frac{1}{(2\pi)^2} \sum_m \int_0^{FBZ} \hbar\omega_m \left| \frac{\partial \omega_m}{\partial \vec{k}} \right| \frac{\partial f(\omega,T)}{\partial T} d\vec{k}, \quad (1)$$

where $f(\omega,T)$ is the Bose-Einstein distribution that describes the phonon occupation and the integral is evaluated over the entire first Brillouin zone for each mode (m). Since our computational resources allow us to compute only a limited number of modes within a reasonable time, we typically evaluate 500 to 2000 eigenfrequencies. In structures of realistic size (e.g. a = 160 nm), these eigenfrequencies cover the range of 0 – 100 GHz, which is only sufficient to calculate thermal conductance at 0.5 K. Inaccuracy of this calculation is estimated (Appendix B) to be about ± 5% of the obtained thermal conductance. For more details on the simulation flow, see our previous work on hole-based PnCs [7].

III. MODIFICATION OF PHONON DISPERSION

First, to demonstrate how pillars change the phonon dispersion of a silicon membrane, let us consider a pillar-based PnC with aluminum phosphide pillars (a = 160 nm, $h_{Membrane} = h_{Pillar}$ = 80 nm, r / a = 0.4). Figure 2 shows the phonon dispersion of this PnC, together with the dispersion of a silicon membrane of the same thickness but without pillars. In addition, horizontal lines show the eigenfrequencies of the pillars without an underlying membrane. The dispersion of the PnC shows hybridization between the modes of the membrane and the pillars [13]: steep regions, corresponding to the membrane modes, flatten near the frequencies of the LRs in the pillars, whereas the flat regions, corresponding to the pillar modes, steepen as they cross the membrane modes. To show that these LRs literally result in physical confinement of elastic waves in the pillars, we have calculated the center of

elastic energy (ξ) in the vertical axis (*z*) as , where *F* is elastic energy density and the integral is evaluated over volume (*V*) of the unit cell, as proposed in Ref. [5]. This center of elastic energy (ξ) is displayed by the color of the modes in Figure 2. Indeed, the modes in the green steep regions, attributed to the waves in the membrane, are physically located in the membrane (ξ < 0.5), whereas the modes in the dark flat regions, attributed to the LRs, are localized in the pillars (ξ > 0.5).

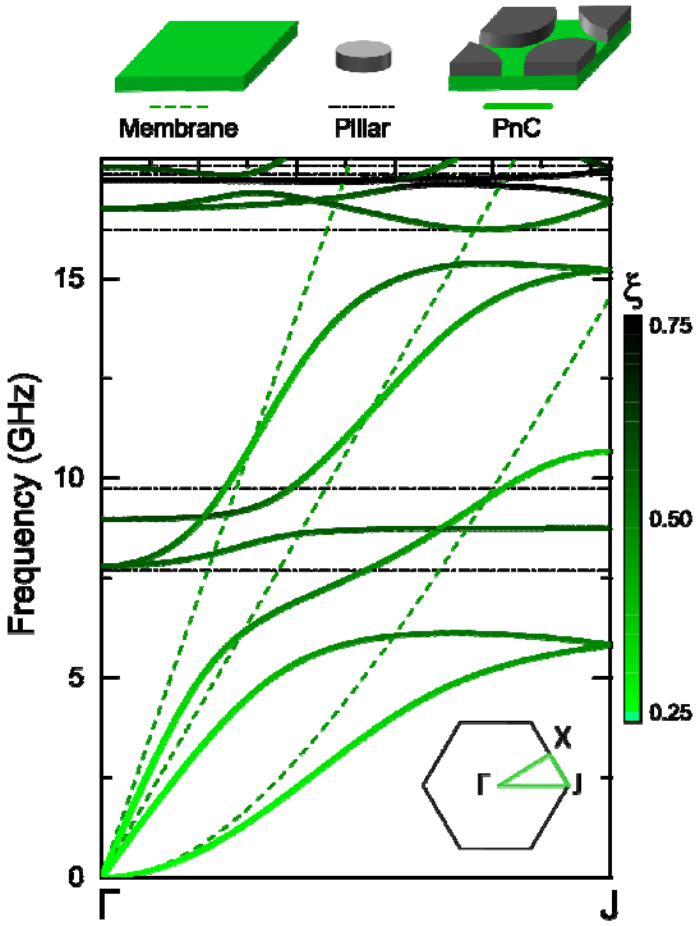

FIG. 2. (Color online) Phonon dispersion of a pillar-based PnC (*a* = 160 nm, *r* / *a* = 0.4, and $h_{Membrane} = h_{Pillar}$ = 80 nm), shown by solid lines, plotted together with the dispersion of a silicon membrane without pillars ($h_{Membrane}$ = 80 nm), shown by green dashed lines, and eigenfrequencies of a single aluminum pillar, shown by black horizontal dash-dotted lines. Color indicates relative height (ξ) of the physical location of the modes.

However, some bands, for example the first, are flattened not by the LRs but rather due to the phonon interference caused by the periodicity of the pillars. Together, these two mechanisms cause a stronger flattening of the phonon dispersion than is observed in hole-based PnCs of the same dimensions [5]. Although such band flattening implies reduction in the group velocity of phonons, the flat regions also cause strong van Hove singularities in the phonon density of states (DOS). To illustrate the changes in the DOS, Figure 3(a) shows the DOS spectra of PnCs with aluminum phosphide and diamond pillars plotted together with the frequencies of LRs in corresponding pillars. In the PnC with diamond pillars, the LRs are few and the corresponding peaks do not significantly affect the spectrum, thus the DOS is similar to that of a membrane. However, in the PnC with aluminum phosphide pillars, the numerous peaks caused by the LRs strongly affect the spectrum making the DOS much higher than that of the membrane. A similar increase in the DOS has recently been shown in the silicon membranes with periodic tungsten inclusions [28]. Such behavior in the DOS of pillar-based PnCs is qualitatively different from that of hole-based PnCs, in which both the group velocity and DOS are typically reduced [7,23,29]. Instead, in pillar-based PnCs, a reduction in the group velocity competes with an increase in the DOS; it is thus unclear whether overall heat conduction is suppressed or enhanced.

To compare heat conduction in different PnCs quantitatively, we calculate the relative thermal conductance $G_{PnC} / G_{Membrane}$ with G_{PnC} and $G_{Membrane}$ as the values of thermal conductance in a given PnC and in a membrane of the same thickness but without pillars, respectively. For the PnC with aluminum phosphide pillars, for example, we found the reduction in thermal conductance to be 55 ± 3%, as compared to the thermal conductance of the membrane at 0.5 K, which was almost as great as the reduction observed for the corresponding hole-based PnC (~63%) [7].

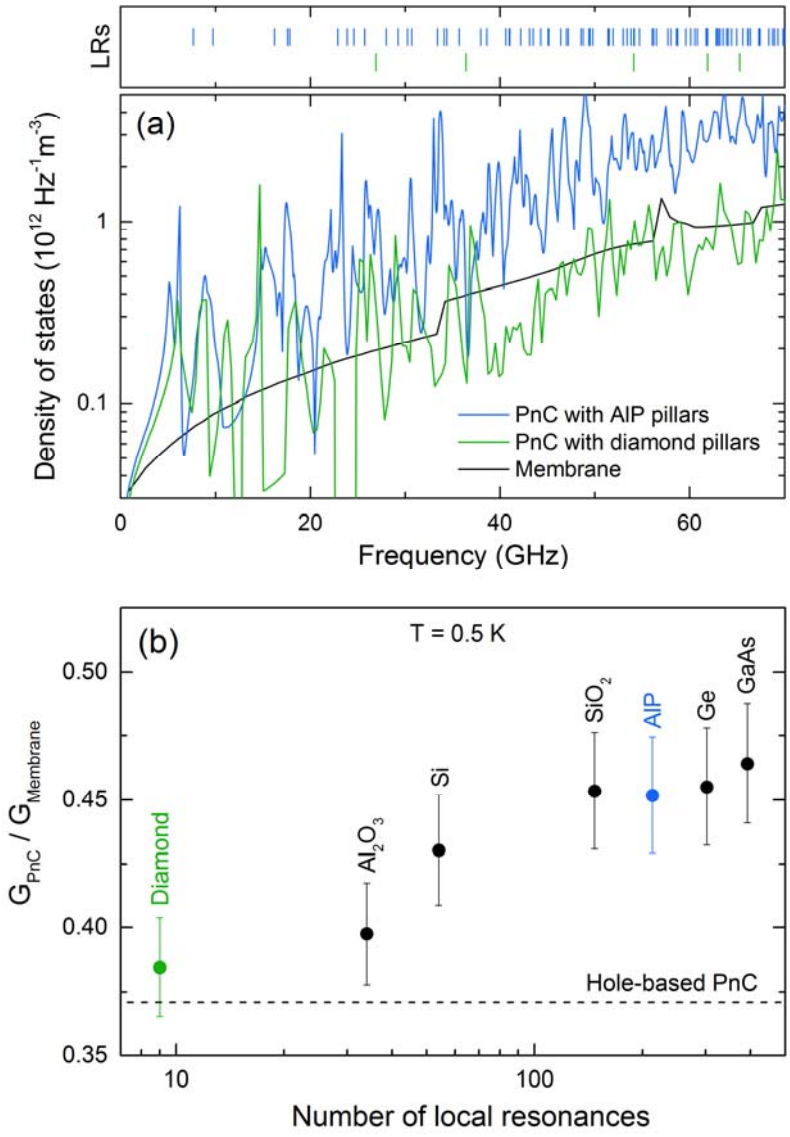

FIG. 3. (Color online). (a) DOS spectra of a silicon membrane and PnCs with aluminum phosphide and diamond pillars (a = 160 nm, r / a = 0.4, and $h_{Pillar} = h_{Membrane}$ = 80 nm). Eigenfrequencies of such pillars without an underlying membrane are plotted in the top panel. (b) Relative thermal conductance of pillar-based PnCs (a = 160 nm, r / a = 0.4, and h = 80 nm) with pillars made of different materials *vs.* number of LRs in phonon spectrum at 0.5 K. The membrane is made of silicon in all the PnCs.

IV. EFFECT OF DIMENSIONS AND MATERIAL

Next, we investigate how the observed reduction in thermal conductance depends on the pillar material and the dimensions of PnCs.

A. Effect of pillar material

Pennec *et al.* [16] showed that the material of both the pillars and membrane changes the phonon dispersion and, particularly, the width of the phononic bandgap. Here, due to the abundance of silicon-on-insulator technology, we use silicon as the material of the membrane and vary the material of the pillars. Figure 3(b) shows that the thermal conductance of PnCs with pillars made of different materials seems to correlate with the expected number of LRs in the pillars of these materials. Indeed, softer pillars have more LRs and thus generate stronger increase in the DOS. However, as the increase in the DOS is partly compensated by the reduction in the group velocity, the thermal conductance changes only slightly, at least for the considered materials, which have relatively few LRs in the spectrum. Nevertheless, should the number of LRs exceed a few hundred, the reduction in group velocity would no longer compensate for the increase in the DOS and the thermal conductance would increase with the number of LRs more steeply. At some point, the pillar-based PnCs could even become more conductive than the membrane without pillars. For example, a PnC with pillars made of PMMA has almost four thousand LRs and shows the 20% higher thermal conductance than the membrane without pillars. Soft metals, such as gold or platinum, could be other examples of materials in which multiple LRs may enhance heat conduction, but since presence of electrons in metals cannot be accounted by the theory of elasticity, metals lie beyond the scopes of this study.

However, these results suggest that LRs seem to contribute to enhancement, rather than reduction, of thermal conductance. Let us now fix aluminum phosphide as the material of the pillars and investigate how different dimensions of the system change the heat conduction and the role of LRs in this process.

B. Effect of pillar height

Another way to demonstrate the effect of LRs on thermal conductance is simply to change the pillar height (h_{Pillar}). Indeed, whereas LRs decrease in frequency as pillar height is increased [12,13,16,17,19],

and thus the number of LRs within a given frequency range will increase with pillar height, the effect of interference caused by periodicity should remain the same [12]. Figure 4 shows that even pillars as short as 15 nm cause a drop of more than 50% in thermal conductance as compared to a membrane without pillars. This drop likely results from the pillar periodicity alone; in such short pillars, the LRs appear at rather high frequencies and are almost absent in the considered frequency range. However, as the pillar height is further increased, the thermal conductance reaches its minimum and starts increasing, because, as the number of LRs exceeds several hundred, the LRs start to increase the DOS. Thus, we see once more that the thermal conductance is lowest in the absence of LRs and only increases in their presence.

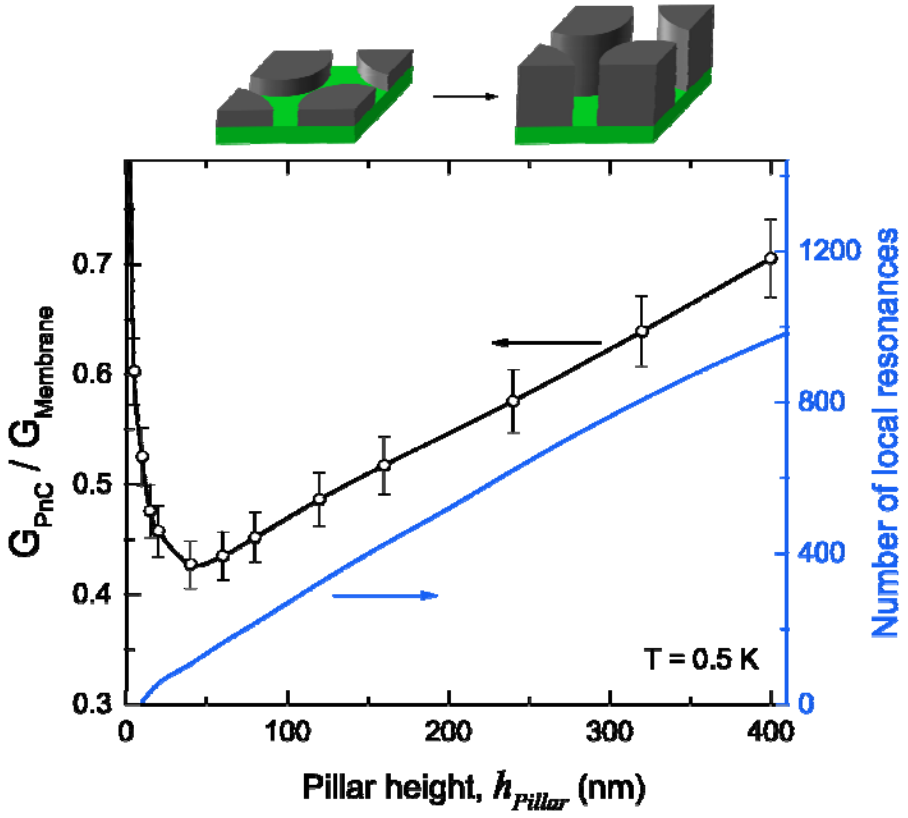

FIG. 4. (Color online). Relative thermal conductance and number of LRs in phonon spectrum at 0.5 K as a function of pillar height (a = 160 nm, r / a = 0.4, and $h_{Membrane}$ = 80 nm).

C. Effect of pillar radius

However, an increase in the DOS due to the LRs does not necessarily cause an increase in thermal conductance. To illustrate, Figure 5 shows the thermal conductance of PnCs with pillars of different radii. Despite the higher number of LRs in pillars of larger radii, thermal conductance decreases as the radius is increased.

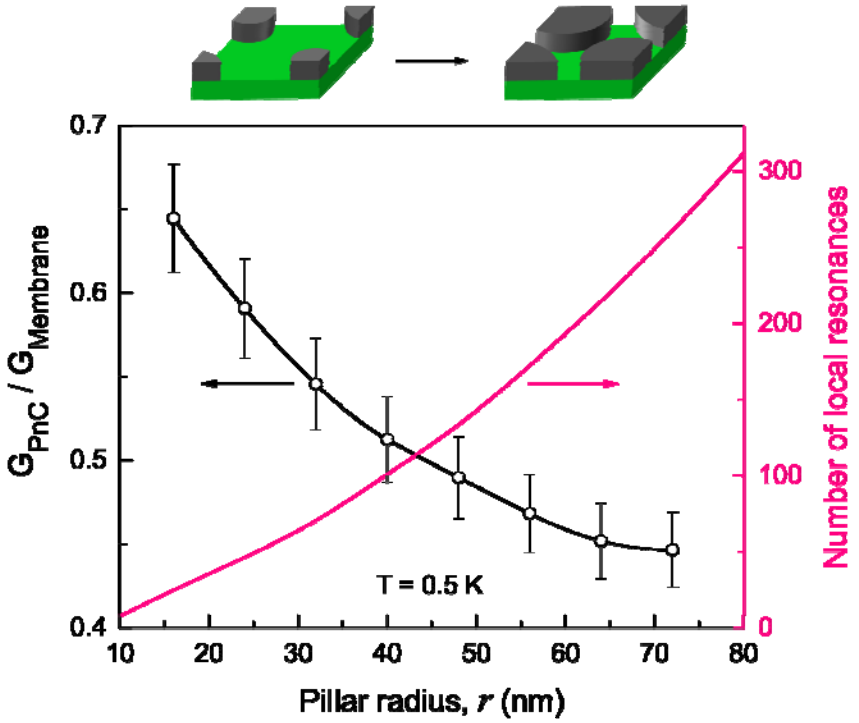

FIG. 5. (Color online). Relative thermal conductance and number of LRs in phonon spectrum at 0.5 K as a function of pillar radius (a = 160 nm and $h_{Membrane} = h_{Pillar}$ = 80 nm).

To understand this result, we should consider changes in both the group velocity and DOS. On one hand, an increase in the r / a ratio reduces group velocities due to the stronger band flattening caused by the periodicity of the structure; this has been shown for hole-based PnCs [7], though band flattening resulting from the LRs also plays a role. On the other hand, unlike in hole-based PnCs, in pillar-based PnCs the DOS increases with the r / a ratio because the number of LRs increases with the pillar size. In the considered PnCs, however, the increase in DOS is not sufficient to overcome the strong reduction in

the group velocity because the number of LRs remains rather small (< 300), resulting in the observed reduction in thermal conductance as the radius is increased. Nevertheless, if the period of the structure or the pillar height had been large enough to introduce a sufficient number of LRs, the radius dependence could have been different.

D. Effect of period and temperature

Experimental [23,30] and theoretical [7,29] studies of hole-based PnCs have shown the strong effect of period (a) and temperature on the reduction in thermal conductance. Here, we investigate their role in pillar-based PnCs and compare the results to the data on the hole-based PnCs [7]. Figure 6(a) shows that both types of PnCs behave alike; however, the existence of LRs in pillar-based PnCs introduces a specific difference. As the period is increased, thermal conductance decreases in both types of PnCs, but whereas the thermal conductance in hole-based PnCs keeps decreasing without an apparent limit [29], the decrease in the pillar-based PnCs seems to be limited. This saturation is caused by the increase in the number of LRs as the pillars become larger along with period (due to the constant r / a ratio). The colors of the points in Figure 6(a) show that the PnCs shorter than 100 nm in period have fewer than 100 LRs at 0.5 K, but the PnC with a period of 320 nm has about 700 LRs, which is sufficient to significantly increase the DOS. Thus, whereas in hole-based PnCs both the DOS and group velocity decrease as period is increased [7,29], in pillar-based PnCs these parameters do not seem to change for periods longer than 160 nm, hence the saturation.

However, when the period is short (< 40 nm at 0.5 K), pillar-based PnCs can demonstrate the "thermal conductance boost effect" [31], i.e. the situation in which PnCs become more conductive than membranes of the same thickness ($G_{PnC} / G_{Membrane} > 1$) as the increase in the DOS overcomes the reduction in group velocity [29,31,32]. For the PnCs with pillars this effect is weaker than in hole-based PnCs, in which the group velocity is generally higher than in pillar-based PnCs. However, should the

pillar material be changed to the one with higher Poisson's ratio, the enhancement of heat conduction can become much stronger.

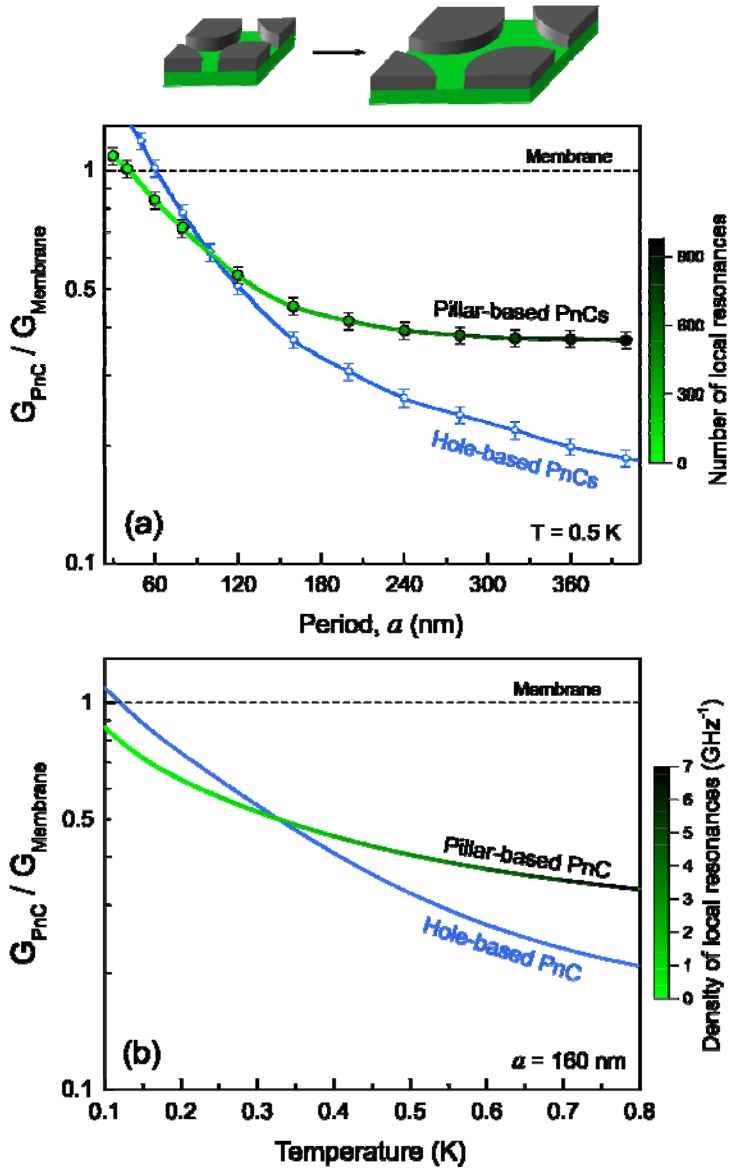

FIG. 6. (Color online). Relative thermal conductance of hole- and pillar-based PnCs (r / a = 0.4 and $h_{Membrane} = h_{Pillar}$ = 80 nm) as a function of (a) the period at 0.5 K and (b) temperature for the period of 160 nm.

A similar enhancement of heat conduction is observed at temperatures below 0.3 K [Fig. 6(b)], at which hole-based PnCs become more conductive than pillar-based PnCs, and even more conductive than a membrane below 0.12 K. As the temperature is increased, phonons at higher frequencies start

contributing to heat conduction in accordance with the Bose-Einstein distribution. In hole-based PnCs, the presence of high-frequency phonons only strengthens the reduction of the thermal conductance, as both the DOS and group velocity decrease at higher frequencies compared to the membrane [7,29]. In pillar-based PnCs, however, the situation at higher frequencies is different: although group velocity also decreases, LRs at higher frequencies become denser, as shown by the color in Figure 6(b), and thus the DOS remains higher than that of the membrane and does not decrease. Therefore, whereas the relative thermal conductance of hole-based PnCs seems to decrease as long as temperature is increased [7,29], in the case of pillar-based PnCs, it remains unclear whether the density of LRs becomes sufficient at some temperature to inverse the trend.

E. Effect of membrane thickness

As far as the thickness of the underlying membrane ($h_{Membrane}$) is concerned, in our previous work [7] we showed that the thickness of hole-based PnCs has nearly no effect on the relative thermal conductance (G_{PnC} / $G_{Membrane}$). However, the situation is different in pillar-based PnCs with thickness below the critical value [33,34], given by $h_c = \hbar\, c_t / 2\, k_B\, T$, with $\hbar$ as the Plank constant, c_t as transversal sound velocity, k_B as Boltzmann constant and T as temperature; at a temperature of 0.5 K, this critical thickness is ~40 nm. In membranes thinner than the critical thickness, phonons occupy only the three lowest branches of the phonon dispersion and the phonon gas becomes quasi two-dimensional [33,34]. Figure 7 shows that at this limit, the thermal conductance of membranes (and hole-based PnCs) is no longer proportional to the thickness, but rather, increases as $1/\sqrt{h_{Membrane}}$ when the thickness is decreased. However, in pillar-based PnCs the thermal conductance remains proportional to the membrane thickness. Hence, the relative thermal conductance is further reduced as the membrane thickness becomes less than the critical thickness, as shown in Figure 7. This phenomenon can serve to

further reduce thermal conductance, especially at ultra-low temperatures at which the critical thickness can reach hundreds of nanometers.

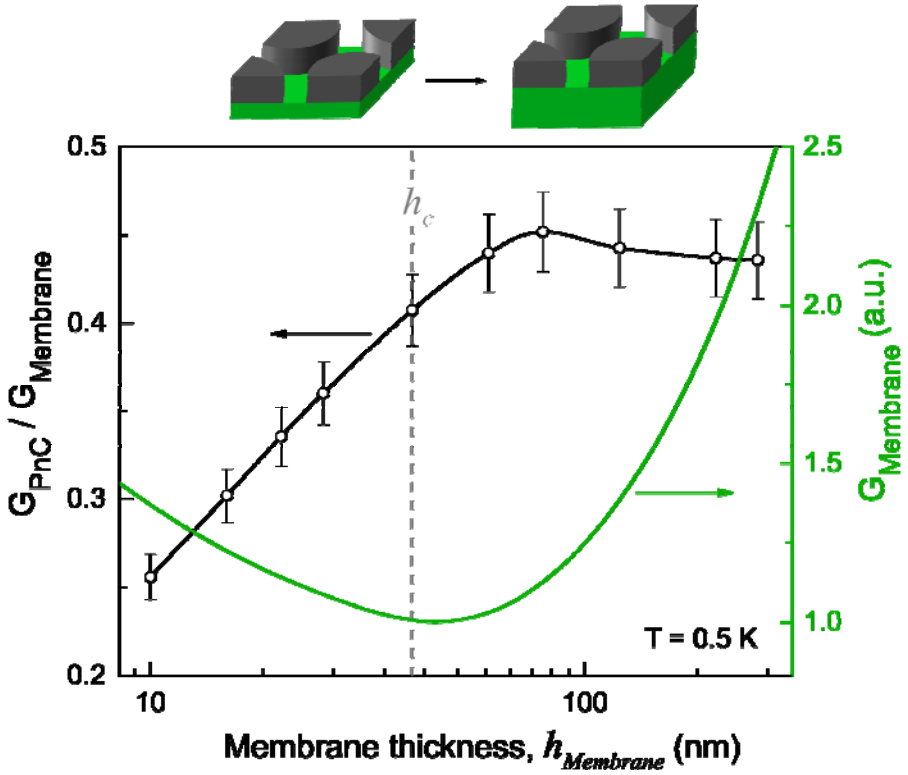

FIG. 7. (Color online). Relative thermal conductance of PnCs (a = 160 nm, r / a = 0.4, and h_{Pillar} = 80 nm) and thermal conductance of membranes as a function of membrane thickness.

E. Effect of lattice

So far, we have only considered pillars in the hexagonal arrangement. Now, let us discuss the effect of the lattice on thermal conductance. In our previous work [7], we concluded that the lattice type does not strongly affect thermal conductance in hole-based PnCs. In pillar-based PnCs, thermal conductance is 10% lower in the honeycomb lattice than in the hexagonal one, and 20% lower in the square lattice, as shown in Figure 8(a). Thus, the effect of the type of the lattice is rather weak as compared to that of the other geometrical parameters.

Nevertheless, we found that the lowest thermal conductivity can be achieved by combining periodic holes and pillars in one PnC. We introduce two types of hybrid hole/pillar-based PnCs, in which a hole (pillar) has been added between the pillars (holes) arranged in a honeycomb lattice, as shown in Figure 8(b). Such hybrid PnCs produce wide acoustic bandgaps [35] and generally have flatter dispersion than either hole- or pillar-based PnCs. Figure 8(a) shows that the thermal conductance in the A type hybrid PnC (pillars in honeycomb lattice) is 24% lower than in the corresponding pillar-based PnC with a honeycomb lattice without holes. The lowest thermal conductance is found in the B type hybrid PnC, where the value is 21% lower than in the corresponding hole-based PnC with a honeycomb lattice without pillars. This additional reduction in hybrid PnCs originates from the strongly reduced group velocity and should be the subject of future investigation.

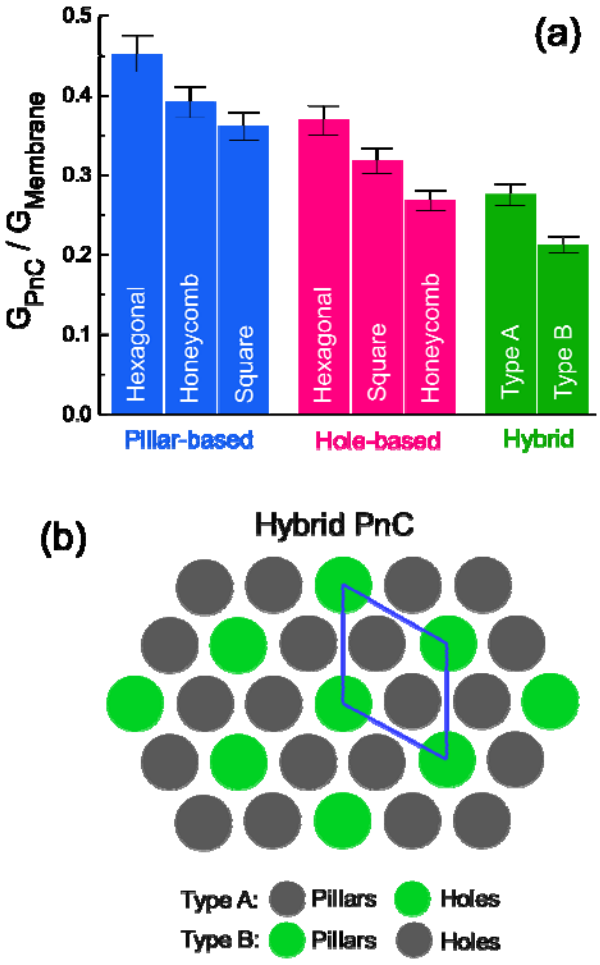

FIG. 8. (Color online). (a) Relative thermal conductance of PnCs of different types and lattices (a = 160 nm, r / a = 0.4, and $h_{Membrane} = h_{Pillar}$ = 80 nm) and (b) schematic of hybrid hole/pillar lattices with indicated unit cell.

V. DISCUSSION AND CONCLUSIONS

In summary, we have studied how various parameters affect heat conduction in pillar-based PnCs of realistic size at sub-Kelvin temperatures in the coherent scattering approximation. We found that the strongest reduction in thermal conductance is achieved when the pillars are rather short and have the maximum possible radius-to-period ratio. The period of the PnCs should generally be long, though saturation in thermal conductance reduction occurs for sufficiently long periods. The thickness of the underlying membrane is unimportant to the reduction in thermal conductance as long as the thickness remains above the critical value; below the critical value, a much stronger reduction is possible. Although the lattice type of PnCs seems to play a minor role, we found that hybrid hole/pillar-based PnCs can reduce thermal conductance below the values for hole- or pillar-based PnCs. As far as LRs in pillars are concerned, we found that LRs increase the DOS and thus contribute to an increase, rather than decrease, in thermal conductance, despite the reduced group velocity. Remarkably, these LRs become a new degree of freedom for heat conduction engineering: thermal conductance of a membrane can be tuned by at least ±50% simply by changing pillar material.

It is interesting to compare our results with those obtained by atomistic simulations of the extremely small pillar-based PnCs widely studied in the literature. On one hand, molecular dynamics simulations predict that even pillars that are only a few atoms short can strongly reduce thermal conductivity [24,25] and that this reduction strengthens as the pillar radius is increased [24], which is consistent with our results. On the other hand, these simulations show nearly no change in thermal conductivity as the pillar height is increased [24,25], contrary to our findings. Such disagreement likely results from not only very

different dimensions and temperatures but also because atomistic simulations consider both coherent and incoherent phonon scattering mechanisms, whereas our model assumes a purely coherent regime. In this regard, some atomistic simulations have demonstrated a strong reduction in phonon mean free path for pillar-based PnCs [26,36]; these studies thus either attributed the reduction in thermal conductivity to the incoherent surface scattering [36,37] or at least admitted such possibility [24,38]. In other words, small pillars may simply act as a surface roughness [37] that scatters phonons randomly.

From this point of view, we can understand other inconsistencies between our results and the results of molecular dynamics simulations. For example, whereas we found that thermal conductance increases as the period of the PnCs is reduced, molecular dynamics simulations predict an opposite trend [24,26,37,39] because, as the structures are scaled down, the ratio of the scattering surfaces to volume increases and thus causes stronger incoherent scattering [40]. As such, although many works explain the suppression of heat conduction in pillar-based PnCs by referencing the LRs and the corresponding reduction in the group velocity [9,24,25,41], incoherent surface scattering might be another possible explanation for these results.

However, it seems clear that properly designed pillar-based PnCs can not only reduce thermal conductance by as much as their hole-based counterparts, but also be even more efficient in some applications. For instance, whereas holes in a membrane reduce both the thermal and electrical conductance of a structure [42–44], pillars are physically outside the membrane and thus should affect only thermal conductance, which is valuable for thermoelectric applications. Moreover, recent advances in nanowire epitaxial growth [45–48] allow the creation of periodic arrays of pillars with desired dimensions and atomically smooth surfaces, whereas periods of few tens of nanometers can be achieved using block-copolymers [49,50]. As such, whereas the fabrication of holes typically results in significant surface roughness that destroys coherence of phonons at rather low temperatures [51,52], in pillar-based PnCs, a low surface roughness can be maintained and thus, phonons can stay coherent at higher

temperatures. This fact makes pillar-based PnCs promising for applications [1,30] involving coherent control of nanoscale heat conduction.

ACKNOWLEDGMENTS

This work was supported by the Project for Developing Innovation Systems of the MEXT, Japan, Kakenhi (15H05869 and 15K13270), PRESTO JST and the Postdoctoral Fellowship of Japan Society for the Promotion of Science. We also thank Prof. Sebastian Volz for helpful discussions.

REFERENCES

[1] M. Maldovan, Nature **503**, 209 (2013).

[2] M. Maldovan, Nat. Mater. **14**, 667 (2015).

[3] M. Maldovan, Phys. Rev. Lett. **110**, 25902 (2013).

[4] B. Kim, J. Nguyena, C. Reinkea, M. Ziaei-Moayyeda, I. El-Kadya, M. S. Drew Goettlerb, Z. C. Lesemanb, and R. H. Olsson III, ECS Trans. **50**, 449 (2012).

[5] B. Graczykowski, M. Sledzinska, F. Alzina, J. Gomis-Bresco, J. S. Reparaz, M. R. Wagner, and C. M. Sotomayor Torres, Phys. Rev. B **91**, 75414 (2015).

[6] M. Sledzinska, B. Graczykowski, F. Alzina, J. Santiso Lopez, and C. M. Sotomayor Torres, Microelectron. Eng. **149**, 41 (2016).

[7] R. Anufriev and M. Nomura, Phys. Rev. B **93**, 45410 (2016).

[8] Y. Achaoui, V. Laude, S. Benchabane, and A. Khelif, J. Appl. Phys. **114**, 104503 (2013).

[9] B. L. Davis and M. I. Hussein, Phys. Rev. Lett. **112**, 55505 (2014).

[10] A. Khelif, Y. Achaoui, and B. Aoubiza, J. Appl. Phys. **112**, 33511 (2012).

[11] A. Khelif, Y. Achaoui, and B. Aoubiza, AIP Adv. **1**, 41404 (2011).

[12] A. Khelif, Y. Achaoui, S. Benchabane, V. Laude, and B. Aoubiza, Phys. Rev. B **81**, 214303 (2010).

[13] R. Pourabolghasem, A. Khelif, S. Mohammadi, A. A. Eftekhar, and A. Adibi, J. Appl. Phys. **116**, 13514 (2014).

[14] Y. Jin, N. Fernez, Y. Pennec, B. Bonello, R. P. Moiseyenko, S. Hémon, Y. Pan, and B. Djafari-Rouhani, Phys. Rev. B **93**, 54109 (2016).

[15] M. Oudich, Y. Li, B. M. Assouar, and Z. Hou, New J. Phys. **12**, 83049 (2010).

[16] Y. Pennec, B. Djafari-Rouhani, H. Larabi, J. O. Vasseur, and A. C. Hladky-Hennion, Phys. Rev. B **78**,

104105 (2008).

[17] T. T. Wu, Z. G. Huang, T. C. Tsai, and T. C. Wu, Appl. Phys. Lett. **93**, 111902 (2008).

[18] Y. Achaoui, A. Khelif, S. Benchabane, L. Robert, and V. Laude, Phys. Rev. B **83**, 104201 (2011).

[19] A. Trzaskowska, S. Mielcarek, and J. Sarkar, J. Appl. Phys. **114**, 134304 (2013).

[20] D. Yudistira, A. Boes, B. Graczykowski, F. Alzina, L. Y. Yeo, C. M. Sotomayor Torres, and A. Mitchell, Phys. Rev. B **94**, 94304 (2016).

[21] M. Addouche, M. A. Al-Lethawe, A. Elayouch, and A. Khelif, AIP Adv. **4**, 124303 (2014).

[22] Y. Pennec, B. Djafari Rouhani, H. Larabi, A. Akjouj, J. N. Gillet, J. O. Vasseur, and G. Thabet, Phys. Rev. B **80**, 144302 (2009).

[23] N. Zen, T. A. Puurtinen, T. J. Isotalo, S. Chaudhuri, and I. J. Maasilta, Nat. Commun. **5**, 3435 (2014).

[24] Z. Wei, J. Yang, K. Bi, and Y. Chen, J. Appl. Phys. **118**, 155103 (2015).

[25] H. Honarvar and M. I. Hussein, Phys. Rev. B **93**, 81412 (2016).

[26] S. Xiong, K. Sääskilahti, Y. A. Kosevich, H. Han, D. Donadio, and S. Volz, Phys. Rev. Lett. **117**, 25503 (2016).

[27] T. Kühn, D. V. Anghel, J. P. Pekola, M. Manninen, and Y. M. Galperin, Phys. Rev. B **70**, 125425 (2004).

[28] A. Arantes and V. Anjos, Model. Simul. Mater. Sci. Eng. **24**, 35017 (2016).

[29] T. A. Puurtinen and I. J. Maasilta, Crystals **6**, 72 (2016).

[30] I. J. Maasilta, T. A. Puurtinen, Y. Tian, and Z. Geng, J. Low Temp. Phys. **184**, 211 (2015).

[31] R. Anufriev and M. Nomura, Phys. Rev. B **91**, 245417 (2015).

[32] A. Arantes and V. Anjos, Model. Simul. Mater. Sci. Eng. **24**, 35017 (2016).

[33] I. J. Maasilta and T. Kühn, J. Low Temp. Phys. **151**, 64 (2008).

[34] T. Kühn and I. J. Maasilta, Nucl. Instruments Methods Phys. Res. Sect. A Accel. Spectrometers, Detect. Assoc. Equip. **559**, 724 (2006).

[35] M. Badreddine Assouar, J. H. Sun, F. S. Lin, and J. C. Hsu, Ultrasonics **54**, 2159 (2014).

[36] S. Neogi, J. S. Reparaz, L. F. C. Pereira, B. Graczykowski, M. R. Wagner, M. Sledzinska, A. Shchepetov, M. Prunnila, J. Ahopelto, C. M. Sotomayor-Torres, and D. Donadio, ACS Nano **9**, 3820 (2015).

[37] Z. Xingli and W. Xiande, Comput. Mater. Sci. **123**, 40 (2016).

[38] Z. Wei, G. Wehmeyer, C. Dames, and Y. Chen, Nanoscale **8**, 16612 (2016).

[39] H. Honarvar, L. Yang, and M. I. Hussein, Appl. Phys. Lett. **108**, 263101 (2016).

[40] R. Anufriev, J. Maire, and M. Nomura, Phys. Rev. B **93**, 45411 (2016).

[41] H. Honarvar, L. Yang, and M. I. Hussein, Appl. Phys. Lett. **108**, 263101 (2016).

[42] J. Lim, H.-T. Wang, J. Tang, S. C. Andrews, H. So, J. Lee, D. H. Lee, T. P. Russell, and P. Yang, ACS Nano **10**, 124 (2016).

[43] M. Nomura, Y. Kage, D. Müller, D. Moser, and O. Paul, Appl. Phys. Lett. **106**, 223106 (2015).

[44] K. Bongsang, J. Nguyena, C. Reinkea, M. Ziaei-Moayyeda, I. El-Kadya, M. S. Drew Goettlerb, Z. C. Lesemanb, and R. H. Olsson III, ECS Trans. **50**, 449 (2012).

[45] Q. Gao, V. G. Dubrovskii, P. Caroff, J. Wong-Leung, L. Li, Y. Guo, L. Fu, H. H. Tan, and C. Jagadish,

Nano Lett. **16**, 4361 (2016).

[46] N. Dhindsa and S. S. Saini, Opt. Lett. **41**, 2045 (2016).

[47] J. P. P. Kakko, T. Haggrén, V. Dhaka, T. Huhtio, A. Peltonen, H. Jiang, E. Kauppinen, and H. Lipsanen, Nano Lett. **15**, 1679 (2015).

[48] F. Kargar, B. Debnath, J.-P. Kakko, A. Säynätjoki, H. Lipsanen, D. L. Nika, R. K. Lake, and A. A. Balandin, Nat. Commun. **7**, 13400 (2016).

[49] A. Checco, A. Rahman, and C. T. Black, Adv. Mater. **26**, 886 (2014).

[50] S. Xiao, X. Yang, E. W. Edwards, Y.-H. La, and P. F. Nealey, Nanotechnology **16**, S324 (2005).

[51] N. K. Ravichandran and A. J. Minnich, Phys. Rev. B **89**, 205432 (2014).

[52] M. R. Wagner, B. Graczykowski, J. S. Reparaz, A. El Sachat, M. Sledzinska, F. Alzina, and C. M. S. Torres, Nano Lett. **16**, 5661 (2016).

[53] H. J. McSkimin, J. Appl. Phys. **24**, 988 (1953).

[54] J. B. Wachtman and D. G. Lam, J. Am. Ceram. Soc. **42**, 254 (1959).

[55] T. A. Puurtinen and I. J. Maasilta, AIP Conf. Proc. **1506**, 9 (2012).

APPENDIX A: MATERIAL PARAMETERS

In this work we used the values of elastic parameters at room temperature because whereas the exact values at 0.5 K are unknown, the values do not seem change significantly as the temperature is decreased below 300 K [53,54].

TABLE 1. Density (ρ), Young's modulus (E), Poisson's ratio (ν) and Lamé parameters (λ and μ) of different materials used in the simulation.

Material	ρ (kg m^{-3})	E (GPa)	ν	λ (GPa)	μ (GPa)
Si	2329	170	0.28	84.45	66.40
AlP	2700	70	0.33	51.08	26.31
Ge	5323	103	0.26	44.28	40.87
GaAs	5316	85.9	0.31	53.49	32.78
Al_2O_3	3965	400	0.22	128.8	163.93
SiO_2	2200	70	0.17	15.41	29.91
Diamond	3515	1050	0.1	119.32	477.27
PMMA	1190	3	0.4	4.29	1.07

APPENDIX B: ERROR ANALYSIS

Three main sources of inaccuracy can affect calculated values of thermal conductance: finite size of elements in the FEM mesh, limited number of calculated wavevectors, and points at which different branches of phonon dispersion intersect.

To estimate the contributions of the size of elements in the FEM mesh, we gradually changed the number of elements in the mesh and determined its effect on thermal conductance at 0.5 K. Figure 9(a) shows that thermal conductance converges as the mesh becomes finer. To obtain the results presented in the paper, we used the meshes with more than 3000 elements, and thus inaccuracy due to the finite element size does not exceed 1 – 2%. Indeed, significant error from this factor can originate only when the considered wavelength is comparable to the element size; in our case, the wavelengths are much longer.

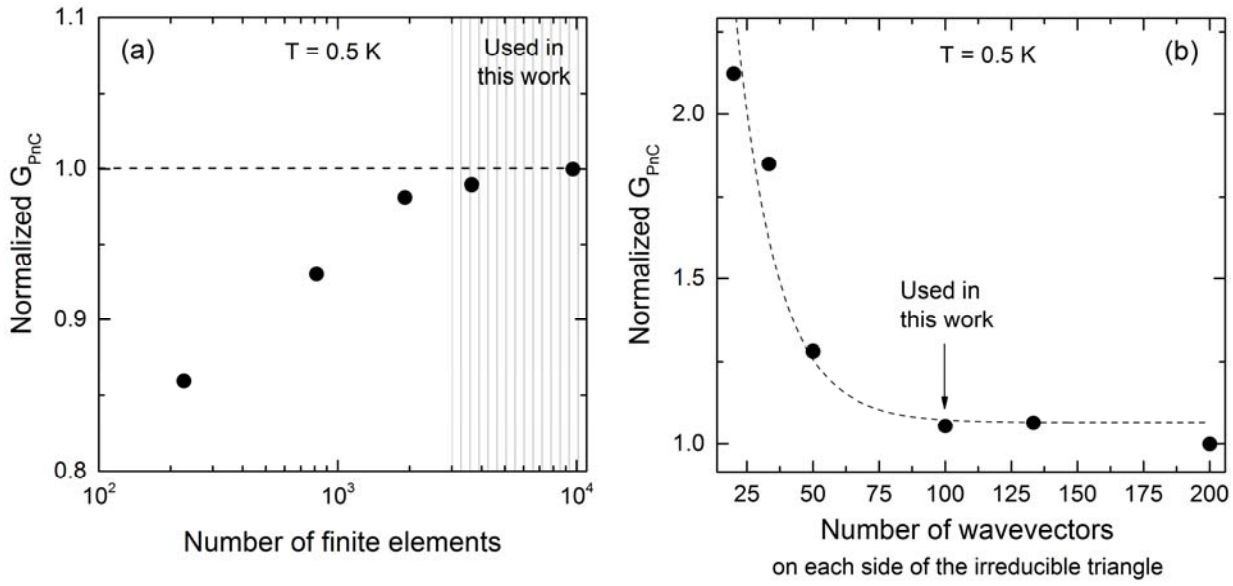

FIG 9. Normalized thermal conductance as a function of (a) number of finite elements in the unite cell and (b) number of the wavevectors on each side of the irreducible triangle.

The second important factor is the number of wavevectors for which the eigenfrequencies were calculated. This number should be sufficiently high to ensure precise derivatives dω/dk. Figure 9(b) shows thermal conductance as a function of the number of wavevectors on each side of the irreducible triangle of the first Brillouin zone. Although small numbers of wavevectors cause large errors, the trend quickly converges when the number of wavevectors is more than 75. Since an increase in the number of wavevectors increases the calculation time proportionally, in our calculations we used 100 wavevectors per triangle side.

Inaccuracy may also originate from the uncertainty in the derivatives dω/dk at the points where different branches of the phonon dispersion seem to intersect. Typical FEM solvers output

eigenfrequencies simply according to the solution number, thus we cannot know whether points across the intersection correspond to the same branch or not. One approach to solving this problem is to evaluate an additional parameter, such as the displacement field or its location, and sort the modes with the condition of continuity of this additional parameter [55]. However, in our case this procedure more than doubled computational time. Therefore, we developed a simplified algorithm that can sort the bands whenever they seem to be intersecting. In reality, however, the actual branches do not always intersect at such points; thus, although our algorithm improves the precision, it does not solve the problem completely. To estimate the remaining error, we changed the assumption from the case where all branches intersect to the cases where only some of them intersect and where they do not intersect at all. We found that the thermal conductance changes in the ± 2% range around an average value.

Thus, we conclude that total inaccuracy in thermal conductivity at 0.5 K is about ± 5% of the value. In addition, there might be a systematic underestimation of thermal conductance due to interpolation of eigenfrequencies, as explained in Appendix C.

APPENDIX C: INTERPOLATION OF EIGENFREQUENCIES

To interpolate the eigenfrequencies inside the irreducible triangle of the first Brillouin zone we rotate the triangle, shown in Fig. 2, clockwise by 120°, so that the J-X side becomes the bottom. Assuming x-y coordinate system with x and y coordinates counted from J point, the eigenfrequencies on the J-X side follow some function $f(x)$ and the eigenfrequencies on the X-Γ side follow some function $g(y)$. Then, the eigenfrequencies inside the triangle are approximated as $F(x, y) = f(x) - f(x)\cdot x/x_{max} + g(y)\cdot x/x_{max}$, where x_{max} is the maximum value of x coordinate (i.e. coordinate of the X point). For a typical structure of $a = 160$ nm at $T = 0.5$ K, this interpolation may result in systematic underestimation of thermal conductance by less than 10 %. However, at very low temperatures or for short periods, this underestimation can become more significant, thus the data in Fig. 6 in the low temperature and short period limits should be used with care.

APPENDIX D: EQUATION FOR THERMAL CONDUCTANCE

In this work we use the same form of the equation for thermal conductance (Eq. 1) as we used in Ref. [7], in order to directly compare the results. Alternatively, one can replace the length of the group velocity vector by the projection of the vector on the direction of the overall heat flux. However, the difference in the ratio of $G_{PnC} / G_{Membrane}$, obtained using these two approaches, does not exceed 6%, thus for the sake of consistency, we decided to keep the same approach as in our previous work. In Ref [31] we took yet another approach to obtain the thermal conductance by multiplication of the group

velocity and DOS spectra; this approach produces significant error of 10 – 20 %, thus the Eq. 1 should be used instead. Moreover, Eq. 1 assumes that temperature of the heat sink is 0 K, thus only the forward heat flux is considered.